Available online at www.sciencedirect.com

SciVerse ScienceDirect

Ceramics International 39 (2013) 315–321

CERAMICS INTERNATIONAL

www.elsevier.com/locate/ceramint

Effects of textural parameters and noble metal loading on the catalytic activity of cryptomelane-type manganese oxides for formaldehyde oxidation

Hua Tian[a], Junhui He[a,*], Linlin Liu[a], Donghui Wang[b]

[a]*Functional Nanomaterials Laboratory and Key Laboratory of Photochemical Conversion and Optoelectronic Materials, Technical Institute of Physics and Chemistry, Chinese Academy of Sciences (CAS), Beijing 100190, China*

[b]*Research Institute of Chemical Defence, Beijing 100083, China*

Received 24 May 2012; received in revised form 8 June 2012; accepted 8 June 2012
Available online 18 June 2012

Abstract

Nanoporous manganese oxides were synthesized by a sol–gel method with maleic acid as an organic reducing agent. Noble metals (Pt and Ag) were then loaded by an impregnation method. The as-prepared materials are tunneled manganese oxides, cryptomelane (K-OMS-2). Further characterization was performed using X-ray diffraction (XRD), transmission electron microscopy (TEM) and N_2 adsorption/desorption techniques. The structure and textural properties are heavily dependent on reaction conditions. Reaction solutions using low temperature produced well-crystallized nanorods, whereas solutions at high temperature yielded poorly-crystallized nanoparticles. Formaldehyde oxidation was carried out to evaluate the catalytic activity of these materials. The cryptomelane nanoparticles that possess higher specific surface area and more open pores showed better catalytic performance than the cryptomelane nanorods. Effects of Pt and Ag on the cryptomelane catalysts indicate that not only noble metal types, but also the existence form of metals on the catalyst surface greatly affects the catalytic activity. Pt/K-OMS-2 consisting of ca. 2 nm Pt nanoparticles presents higher activity than Ag/K-OMS-2, but lower activity than the corresponding cryptomelane materials without metal loading, due to the cover of Pt on the active sites of manganese oxides.

Keywords: Manganese oxides; Cryptomelane; Noble metal; Formaldehyde oxidation

1. Introduction

Cryptomelane-type manganese oxide is a microporous manganese oxide octahedral molecular sieve (OMS-2) with the approximate stoichiometry of KMn_8O_{16} and a tunnel structure [1]. Cryptomelane contains mixed-valence manganese from Mn^{4+} to Mn^{2+}. K^+ resides in the tunnel along with small amounts of water for stabilizing the $0.46 \times 0.46\ nm^2$ tunnel structure [2]. Because of its unique physical and chemical properties, K-OMS-2 materials exhibit excellent catalytic performance, and have attracted a far amount of attention in recent years.

Formaldehyde (HCHO) is one of the major indoor air pollutants emitted from widely used constructive and decorative materials. Long-term exposure to formaldehyde that exceeds safe concentration may cause adverse effects on human health including lethiferous diseases [3]. To meet these challenges, various techniques have been explored. Catalytic oxidation has been proved to be an effective method for combating formaldehyde pollution [4,5]. Manganese oxide is one of excellent catalysts reported so far for formaldehyde oxidation. For instance, manganese oxides with tunnel structure have been reported to possess high catalytic activity in formaldehyde oxidation at low temperature [6,7]. However, the operating temperature for these catalysts is still high for practical applications. To enhance their catalytic activity, noble metals have been incorporated and shown good catalytic performance at moderate temperature [8–10].

*Corresponding author. Tel./fax: +86 10 82543535.
E-mail address: jhhe@mail.ipc.ac.cn (J. He).

0272-8842/$36.00
http://dx.doi.org/10.1016/j.ceramint.2012.06.027

Tang et al. [9] found that the addition of Ag promoted complete oxidation of formaldehyde at a lower temperature of 140 °C than pure MnO_x, over which the complete oxidation of formaldehyde into H_2O and CO_2 was not achieved even at 200 °C. Álvarez-Galván et al. [11] reported that the 18.2% MnO_x/Al_2O_3 catalysts produced total oxidation of formaldehyde at 220 °C, but this temperature could decrease to 90 °C when 0.1% Pd was incorporated into this catalyst.

Recently, remarkable research has been concentrated on investigating the catalytic performance of oxide-supported Pt catalysts for formaldehyde oxidation. These Pt-based catalysts exhibit extraordinarily high activity even at room temperature [12,13]. For instance, Tang et al. [13] reported that the Pt/MnO_x–CeO_2 catalysts prepared from $Pt(NH_3)_2(NO_2)_2$ showed high activity, over which formaldehyde could be completely oxidized into CO_2 and H_2O at ambient temperature. But the bare support only gave 26% of formaldehyde conversion under the same reaction conditions. An et al. [14] found a Pt/Fe_2O_3 catalyst calcined at 300 °C could completely oxidize 200 ppm of formaldehyde at room temperature and exhibited excellent stability. Wang and Li [15] investigated the effect of Pt on catalytic performance of OMS-2 catalysts. Interestingly, they demonstrated that the loading of Pt did not change the complete oxidation temperature of formaldehyde, just decreased the ignition temperature of formaldehyde oxidation and promoted the formaldehyde oxidation at lower temperature. The parameters of the catalyst structure determined the temperature of complete oxidation of formaldehyde. These results reported by Wang and co-workers are much different from the other reported, possibly due to the unique $0.46 \times 0.46\ nm^2$ tunnels in the OMS-2 structure.

Herein, we present a series of cryptomelane materials prepared by a sol–gel route. Cryptomelane supported Ag and Pt catalysts were also obtained using an impregnation method. Crystallographic, morphological and other properties of the products synthesized at different reaction temperatures were investigated to study the relationship between textural parameters of catalysts and their catalytic performances. The formaldehyde conversions over noble metals (Ag and Pt) loaded catalysts were also compared.

2. Experimental

2.1. Chemicals

All chemicals in this study were of commercially available analytical grade and used without further purification. All reactions were carried out using deionized water (18 MΩ) from a Millipore Milli-Q Plus 185 purifying system.

2.2. Cryptomelane synthesis

The cryptomelane materials investigated in the current work were synthesized via a sol–gel reaction. In a typical synthesis, maleic acid (0.78 g, 6.7 mmol) and $KMnO_4$ (3.16 g, 20 mmol) were dissolving in deionized water (200 mL) at predetermined temperatures (15–70 °C). After stirring for 30 min, the mixture was allowed to settle for 60 min. The sample obtained after this step was then filtered, washed with deionized water, and dried at 110 °C for 12 h. Then calcination was carried out at 450 °C for 2 h. The product was pulverized, washed with 0.1 M HCl and deionized water, and then dried at 110 °C for 12 h. The obtained product is denoted as K-OMS-2.

3 wt% Ag-loaded and 1 wt% Pt-loaded cryptomelane catalysts were synthesized by the conventional impregnation process. The cryptomelane powder (prepared at 15 °C) was added to an aqueous solution of $AgNO_3$ or H_2PtCl_6, followed by stirring for 6 h. After that the mixtures were dried at 100 °C for 6 h and calcined at 250 or 400 °C for 2 h. These catalysts are designated as Ag/K-OMS-2 and Pt/K-OMS-2, respectively.

2.3. Characterization

X-ray powder diffraction (XRD) analysis was conducted on a Bruker D8 Focus diffractometer with a Cu Kα X-ray source (40 mA, 40 kV). The morphologies of the products were studied by transmission electron microscopy (TEM) on a JEOL JEM-2100F electron microscope. The chemical compositions were determined by energy-dispersive X-ray analysis (EDX) employing a 6853-H (Horiba Instruments) spectrometer and reported in atomic weight percentages. Textural properties were studied with a Quadrasorb SI automated surface area and pore size analyzer. Before acquiring nitrogen adsorption and desorption isotherms at 77 K, samples were degassed at 100 °C under vacuum for 12 h. The specific surface area and pore size distribution were calculated according to the Braunauer–Emmett–Teller (BET) and Barrett–Joyner–Halenda (BJH) methods.

2.4. Catalytic studies

The formaldehyde catalytic oxidation was performed in a fixed-bed reactor (i.d. 4 mm) loaded with 100 mg of the catalyst. The reaction mixture containing 460 ppm formaldehyde, 21 vol% O_2 and the balance gas (N_2). The total flow rate was 50 mL min^{-1} in a space velocity of 30,000 mL g_{cat}^{-1} h^{-1}. The effluents from the reactor were analyzed with an on-line Agilent 6890 gas chromatograph equipped with FID and Ni catalyst converter which was used for converting carbon oxides quantitatively into methane in the presence of hydrogen before the detector. Conversion was expressed in the yield of CO_2 of the effluent, and calculated as follows:

$$CO_2\ \text{yield}\ (\%) = \frac{[CO_2]_{out}\ \text{vol}\%}{[HCHO]_{in}\ \text{vol}\%} \times 100,$$

where $[CO_2]_{out}$ is the CO_2 concentration in the products (vol%), and $[HCHO]_{in}$ is the formaldehyde concentration in the feed gas (vol%).

3. Results and discussion

3.1. Features of materials

XRD was used to identify the phases of the samples and to determine the effect of synthesis temperature on the crystallization of K-OMS-2. As shown in Fig. 1, all of the peaks for the sample synthesized at 15 °C match the reference data of a pure cryptomelane phase [16]. Synthesis temperature is found to dramatically influence the crystallinity of products. When the synthesis temperature is increased from 15 to 40 °C, the XRD pattern intensity of the product increases slightly. But as the temperature is increased to 70 °C, the product is less crystalline. This phenomenon has not been reported for cryptomelane manganese oxides prepared by sol–gel method. As already known, raising synthesis temperature can increase the reaction rate, and gels are formed more rapidly [17], leading to increase of crystallinity of products. However, too high temperature of the synthesis diminishes the thermal stability of gels, and amorphous materials are produced.

The phase purity of the noble metal-loaded K-OMS-2 was also investigated by XRD, as shown in Fig. 2. The XRD patterns are in excellent agreement with those of cryptomelane materials. No additional peaks corresponding to segregated crystalline phases of Ag and Pt were observed, indicating that Ag and Pt species have a very high dispersion degree or has too low amount to be detected.

Morphological studies on the products were conducted by TEM. Fig. 3 shows typical morphologies of the selected K-OMS-2 and noble metal-loaded samples. The sample of K-OMS-2 prepared at 15 °C shows nanorods of diameters ranging from 20 to 50 nm. With increasing the synthesis temperature to 70 °C, agglomerated nanoparticles with an average size of ca. 10 nm were obtained. This is an amorphous phase, as confirmed by the XRD pattern. Materials in Fig. 3(c) and (d) have the similar nanorod

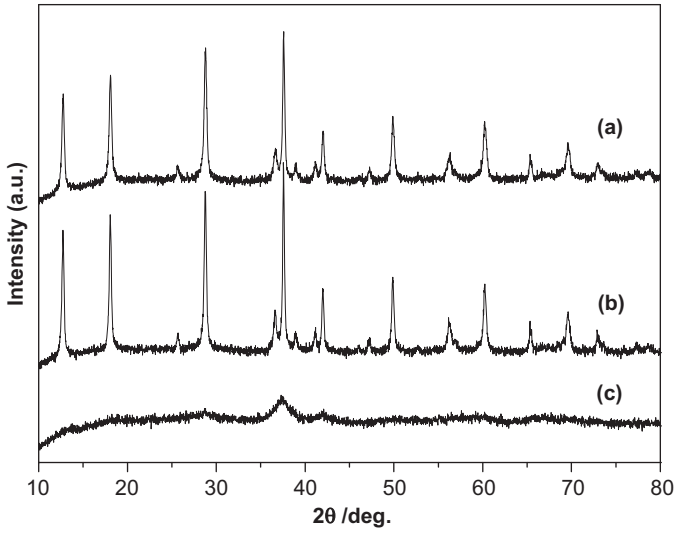

Fig. 1. XRD patterns of K-OMS-2 materials synthesized at 15 °C (a), 40 °C (b) and 70 °C (c).

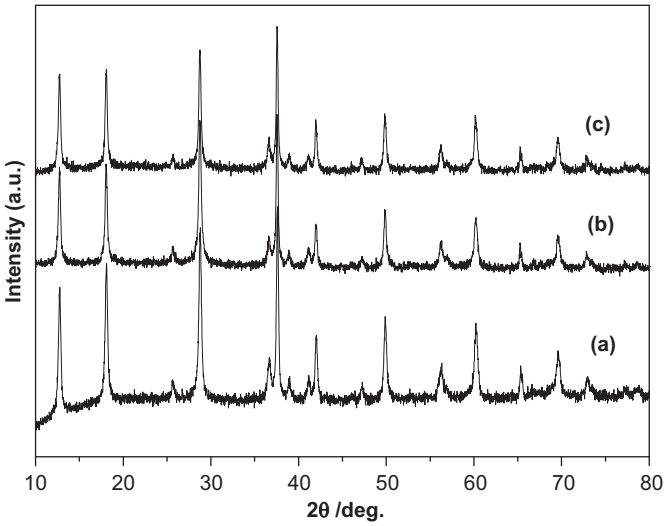

Fig. 2. XRD patterns of K-OMS-2 and its metal-loaded products. (a) K-OMS-2; (b) Ag/K-OMS-2 and (c) Pt/K-OMS-2.

morphologies as the unloaded K-OMS-2, but have longer lengths after the addition of Pt. Ag species is characterized as dispersed nanoparticles with a particle size of ca. 10 nm, without significant aggregation. High-resolution TEM image in Fig. 3(d) clearly shows that Pt nanoparticles have a significantly smaller particle size of ca. 2 nm and are well dispersed on the frameworks of cryptomelane tunnels. Apart from the promotion of the migration/exchange of the oxygen species, the mutual interaction of noble metal and support material influences the reactive sites of catalyst [18]. Therefore, this existence form of the supported noble metal would affect the catalytic activity of catalyst.

The chemical compositions of the as-prepared products were determined using the EDX method, and the results are summarized in Table 1. It is indicated that the Ag and Pt were successfully loaded in the cryptomelane materials. The atomic weight percentages of Ag and Pt in the K-OMS-2 samples are 3.27 and 1.52 wt%, respectively, just slightly greater than their initial calculated values of 3 and 1 wt%.

The N_2 adsorption/desorption isotherms of K-OMS-2 materials are shown in Fig. 4. The K-OMS-2 nanorods prepared at 15 and 40 °C show type II adsorption isotherms at low P/P_0. The hysteresis loops in the P/P_0 range above 0.5 are typical type H3 adsorption isotherms, suggesting the presence of slit-shaped mesopores with nonuniform sizes, probably due to the aggregation of particles. Notably, when the synthesis temperature increases to 70 °C, the N_2 adsorption/desorption isotherm and its corresponding hysteresis loop are quite different from those reported for regular cryptomelane materials [19,20]. The isotherm exhibits an IV-type curve according to the IUPAC classification of adsorption isotherms [21], and an obviously large hysteresis loop of type H1 appears [22,23], indicating uniform mesopores. This phenomenon probably originates from the small particle size and narrow mesopore size distribution of the K-OMS-2 nanoparticles prepared at 70 °C.

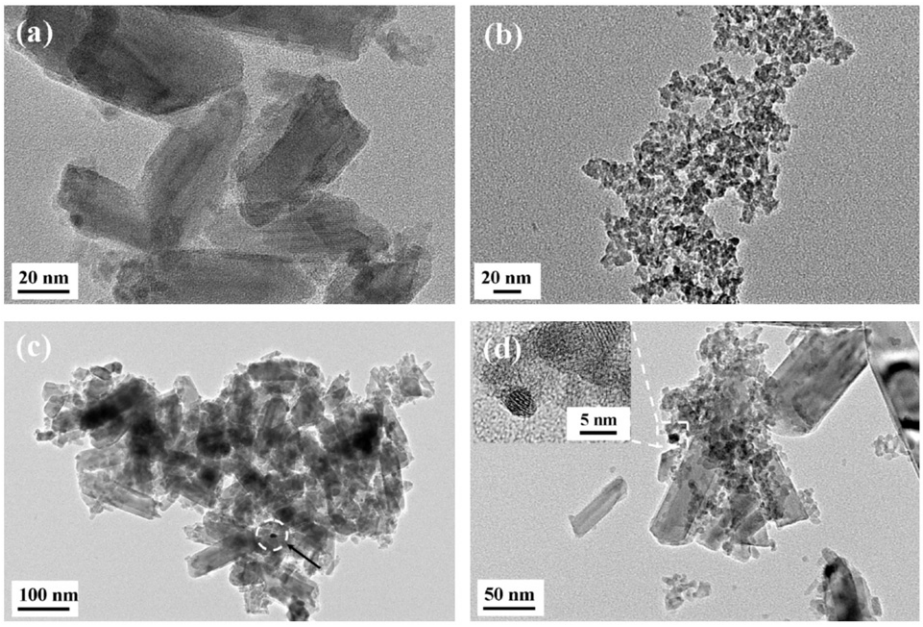

Fig. 3. TEM images of K-OMS-2 and its metal-loaded products. (a) K-OMS-2 (15 °C); (b) K-OMS-2 (70 °C); (c) Ag/K-OMS-2 and (d) Pt/K-OMS-2.

Table 1
Chemical analysis for K-OMS-2 and its metal-loaded products.

Sample	Composition (wt%)		
	K	Mn	Metal loading
K-OMS-2	4.95	67.45	–
Ag/K-OMS-2	3.87	54.96	3.27
Pt/K-OMS-2	4.37	62.19	1.52

Table 2
Textural properties of prepared K-OMS-2 materials.

Temperature (°C)	SBET ($m^2\ g^{-1}$)	Vp[a] ($cm^3\ g^{-1}$)	Dp[b] (nm)
15	68	0.20	12
40	68	0.22	13
70	206	0.30	6

[a]Total pore volumes obtained at $P/P_0=0.99$.
[b]Pore size determined from the desorption branch using the BJH method.

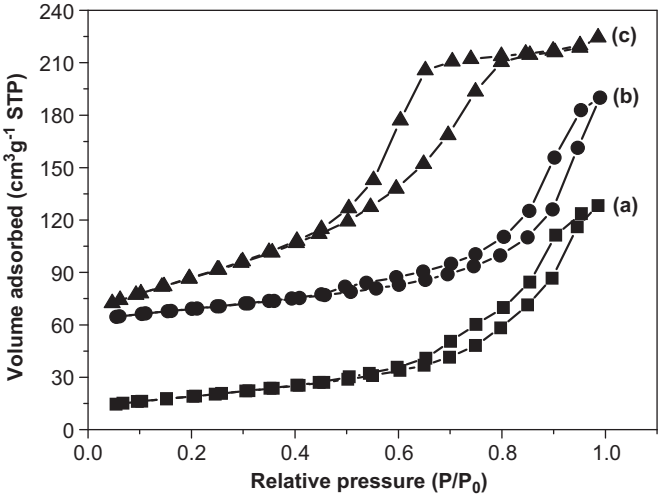

Fig. 4. N_2 adsorption/desorption isotherms of K-OMS-2 materials: (a) K-OMS-2 (15 °C), (b) K-OMS-2 (40 °C), and (c) K-OMS-2 (70 °C).

Textural properties of K-OMS-2 samples are listed in Table 2. It can be seen that increase in the synthesis temperature from 15 to 40 °C does not improve the sample specific surface area but slightly increases the pore volume from 0.20 to 0.22 $cm^3\ g^{-1}$ and the pore diameter from 12 to 13 nm. It appears that the synthesis temperature lower than 40 °C does not have much influence on the textural properties. However, as the temperature is raised to 70 °C, the specific surface area increases dramatically to 206 $m^2\ g^{-1}$. The pore diameter of K-OMS-2 sample obtained at 70 °C is found to be smaller than the other two materials. These results match the XRD data (Fig. 1) and TEM images (Fig. 3) in terms of the particle size, as the further high synthesis temperature of 70 °C leads to a significant change in morphology and great decrease in particle size, which is accompanied by an increase in the specific surface area.

3.2. Catalytic activity

Catalytic activity of K-OMS-2 samples prepared at different temperatures was evaluated in the formaldehyde oxidation reaction, and the results are showed in Fig. 5. Data obtained reveal that the synthesis temperature greatly influences the catalytic performances. Evidently formaldehyde oxidation proceeds more effectively over the K-OMS-2

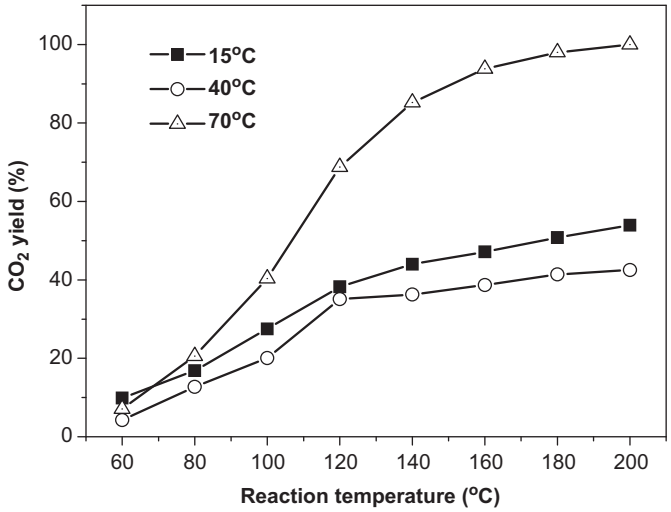

Fig. 5. Effect of the synthesis temperature on the catalytic activity of K-OMS-2 catalysts.

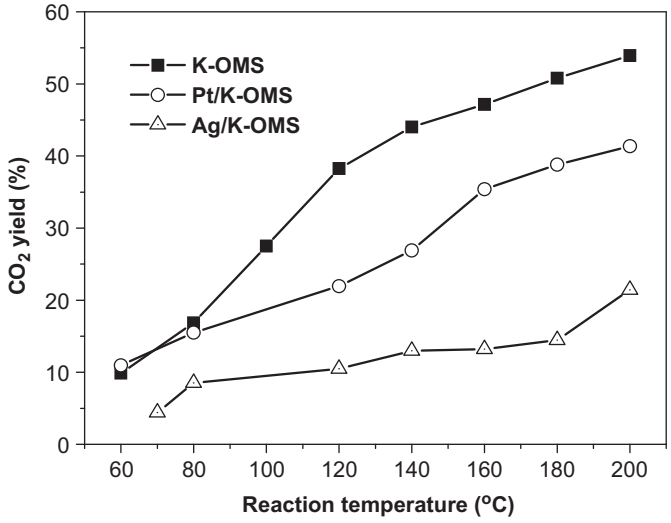

Fig. 6. Performances of K-OMS-2 and metal-loaded catalysts in formaldehyde conversion.

catalyst obtained at 70 °C, and 100% of CO_2 yield from the formaldehyde decomposition is achieved at 200 °C. Whereas the samples prepared at 15 and 40 °C only give the CO_2 yields of ca. 54% and 42%, respectively, under the same conditions. As mentioned above, the temperature elevation for preparing K-OMS-2 catalyst results in a dramatic increase in the specific surface area and the formation of nanoparticles with small sizes, leading to a large increase of surface active sites and more accessible pore channels of K-OMS-2 for the adsorption and diffusion of formaldehyde molecules. As a result, the activity increases significantly.

Fig. 6 presents the catalytic activity of pure K-OMS-2 and noble metal-loaded catalysts. Clearly, the formaldehyde conversion strongly depends on the type of supported noble metal. The Pt/K-OMS-2 catalyst exhibits higher activity than the Ag/K-OMS-2 catalyst. This result is similar to those reported for regular Pt and Ag supported catalysts. Previous studies suggested that the addition of noble metals such as Pt and Ag could highly improve the catalytic performance in formaldehyde oxidation, and Pt supported catalyst was much more effective than Ag supported materials [9,13]. However, as shown in Fig. 6, after Pt- or Ag-loading, the catalytic activity decreases and thus the CO_2 yield drops from 54% to 41% and 21% respectively at the reaction temperature of 200 °C.

3.3. Discussion

It is known that the catalytic activity of noble metal-loaded catalysts for the oxidation of formaldehyde and other volatile organic compounds is influenced by a combination of factors including preparation method, specific surface area, type and particle size of noble metal, and the location of noble metal on support materials [24–27]. Pt/K-OMS-2 and Ag/K-OMS-2 used in this work were prepared by the conventional impregnation method as those used for other Pt and Ag loading catalysts reported elsewhere. Meanwhile, Pt and Ag nanoparticles are well dispersed on the K-OMS-2 materials and typically small. Therefore, the decrease in catalytic activity of these catalysts cannot be significantly attributed to the effects of the preparation method and the particle size of noble metal.

As shown in Fig. 6, the support material, cryptomelane manganese oxide itself shows high activity for formaldehyde oxidation. Furthermore, different from support materials of other noble metal-loaded catalysts, such as MnO_x, CeO_2 and so on [9,13], the current support has a tunnel structure consisting of two edge-shared MnO_6 octahedra on each side (2×2), exhibiting easy release of lattice oxygen and acidic sites [28]. The dynamic diameter value of formaldehyde is 0.24 nm [29], very close to that of effective diameter (ca. 0.26 nm) of cryptomelane tunnels calculated by electron-density distribution [30]. Based on these, the support structure and the location of the loaded noble metal seem to be among the major factors contributing to the activity of catalysts in the formaldehyde oxidation reaction. Fig. 3 reveals that Pt and Ag nanoparticles are well dispersed on the surface of K-OMS-2 nanorods. High-resolution TEM image clearly shows that the Pt nanoparticles are distributed evenly over the entire surface of the framework of K-OMS-2 catalyst. This existence form of noble metals would significantly cover the surface acidic sites and active sites of manganese oxide catalysts [31]. Though the addition of Pt and Ag could lead to the formation of lattice defects in which mobility of oxygen species can be greatly promoted, the influence of decreasing active sites seems to be relatively higher in the current research [15]. Thus, for noble metal-loaded catalysts, especially for those with highly active support, the textural properties of support materials and the existence form of noble metal nanoparticles have significant effects on the formaldehyde oxidation reaction.

4. Conclusions

We have demonstrated a facile sol-gel route to tailoring the crystallinity, morphology, specific surface area and pore structure, and hence the catalytic activity of cryptomelane manganese oxides. K-OMS-2 with high specific surface area of 206 $m^2 g^{-1}$, ultrafine particles of ca. 10 nm and uniform mesopores were obtained at 70 °C, and it exhibited excellent catalytic activity for formaldehyde oxidation compared with those synthesized at lower temperatures. Pt and Ag loaded K-OMS-2 catalysts were synthesized by an impregnation method. Pt/K-OMS-2 showed higher activity than Ag/K-OMS-2 in the formaldehyde oxidation reaction, but showed degraded performance compared to the unloaded K-OMS-2 catalyst, which is quite different from those reported for regular noble metal-loaded catalysts. Thus, not only noble metal types, but also the support structure and the existence form of the loaded noble metals exhibit significant influence on the formaldehyde oxidation. The insights obtained in this work would inspire further researches into the design and synthesis of novel noble metal catalysts suitable for low-temperature catalytic oxidation of formaldehyde and other organic pollutants.

Acknowledgments

This work was financially supported by the National Natural Science Foundation of China (20871118, 21007076).

References

[1] R.N. DeGuzman, Y.F. Shen, E.J. Neth, S.L. Suib, C.-L. O'Young, S. Levine, J.M. Newsam, Synthesis and characterization of octahedral molecular sieves (OMS–2) having the hollandite structure, Chemistry of Materials 6 (1994) 815–821.

[2] S. Ching, J. Roark, N. Duan, S.L. Suib, Sol–gel route to the tunneled manganese oxide cryptomelane, Chemistry of Materials 9 (1997) 750–754.

[3] IARC, Formaldehyde, 2-butoxyethanol and 1-tert–butoxypropan-2-ol, Monographs on the evaluation of carcinogenic risks to humans 88 (2006).

[4] J. Zhang, Y. Jin, C. Li, Y. Shen, L. Han, Z. Hu, X. Di, Z. Liu, Creation of three-dimensionally ordered macroporous Au/CeO_2 catalysts with controlled pore sizes and their enhanced catalytic performance for formaldehyde oxidation, Applied Catalysis B 91 (2009) 11–20.

[5] C. Ma, D. Wang, W. Xue, B. Dou, H. Wang, Z. Hao, Investigation of formaldehyde oxidation over Co_3O_4–CeO_2 and Au/Co_3O_4–CeO_2 catalysts at room temperature: effective removal and determination of reaction mechanism, Environmental Science & Technology 45 (2011) 3628–3634.

[6] T. Chen, H. Dou, X. Li, X. Tang, J. Li, J. Hao, Tunnel structure effect of manganese oxides in complete oxidation of formaldehyde, Microporous and Mesoporous Materials 122 (2009) 270–274.

[7] H. Tian, J. He, X. Zhang, L. Zhou, D. Wang, Facile synthesis of porous manganese oxide K-OMS-2 materials and their catalytic activity for formaldehyde oxidation, Microporous and Mesoporous Materials 138 (2011) 118–122.

[8] V.A. de la Peña O'Shea, M.C. Alvarez-Galván, J.L.G. Fierro, P.L. Arias, Influence of feed composition on the activity of Mn and $PdMn/Al_2O_3$ catalysts for combustion of formaldehyde/methanol, Applied Catalysis B 57 (2005) 191–199.

[9] X. Tang, J. Chen, Y. Li, Y. Li, Y. Xu, W. Shen, Complete oxidation of formaldehyde over Ag/MnO_x–CeO_2 catalysts, Chemical Engineering Journal 118 (2006) 119–125.

[10] Y.C. Hong, K.Q. Sun, K.H. Han, G. Liu, B.Q. Xu, Comparison of catalytic combustion of carbon monoxide and formaldehyde over Au/ZrO_2 catalysts, Catalysis Today 158 (2010) 415–422.

[11] M.C. Álvarez-Galván, B. Pawelec, V.A. de la Peña O'Shea, J.L.G. Fierro, P.L. Arias, Formaldehyde/methanol combustion on alumina-supported manganese–palladium oxide catalyst, Applied Catalysis B 51 (2004) 83–91.

[12] C. Zhang, H. He, K. Tanaka, Catalytic performance and mechanism of a Pt/TiO_2 catalyst for the oxidation of formaldehyde at room temperature, Applied Catalysis B 65 (2006) 37–43.

[13] X. Tang, J. Chen, X. Huang, Y. Xu, W. Shen, Pt/MnO_x–CeO_2 catalysts for the complete oxidation of formaldehyde at ambient temperature, Applied Catalysis B 81 (2008) 115–121.

[14] N. An, Q. Yu, G. Liu, S. Li, M. Jia, W. Zhang, Complete oxidation of formaldehyde at ambient temperature over supported Pt/Fe_2O_3 catalysts prepared by colloid-deposition method, Journal of Hazardous Materials 186 (2011) 1392–1397.

[15] R. Wang, J. Li, OMS-2 catalysts for formaldehyde oxidation: effects of Ce and Pt on structure and performance of the catalysts, Catalysis Letters 131 (2009) 500–505.

[16] C.K. King'ondu, N. Opembe, C.H. Chen, K. Ngala, H. Huang, A. Iyer, H.F. Garces, S.L. Suib, Manganese oxide octahedral molecular sieves (OMS-2) multiple framework substitutions: a new route to OMS-2 particle size and morphology control, Advanced Functional Materials 21 (2011) 312–323.

[17] N. Duan, S.L. Suib, C.L. O'Young, Sol–gel synthesis of cryptomelane, an octahedral molecular sieve, Journal of the Chemical Society Chemical Communications 13 (1995) 1367–1368.

[18] Z. Abbasi, M. Haghighi, E. Fatehifar, S. Saedy, Synthesis and physicochemical characterizations of nanostructured Pt/Al_2O_3–CeO_2 catalysts for total oxidation of VOCs, Journal of Hazardous Materials 186 (2011) 1445–1454.

[19] N.N. Opembe, C.K. King'ondu, A.E. Espinal, C.H. Chen, E.K. Nyutu, V.M. Crisostomo, S.L. Suib, Microwave-assisted synthesis of manganese oxide octahedral molecular sieve (OMS-2) nanomaterials under continuous flow conditions, Journal of Physical Chemistry C 114 (2010) 14417–14426.

[20] I. Atribak, A. Bueno–Lopez, A. Garcia–Garcia, P. Navarro, D. Frias, M. Montes, Catalytic activity for soot combustion of birnessite and cryptomelane, Applied Catalysis B 93 (2010) 267–273.

[21] J.J. Li, X.Y. Xu, Z. Jiang, Z.P. Hao, C. Hu, Nanoporous silica-supported nanometric palladium: synthesis, characterization, and catalytic deep oxidation of benzene, Environmental Science & Technology 39 (2005) 1319–1323.

[22] L.B. Sun, J.H. Kou, Y. Chun, J. Yang, F.N. Gu, Y. Wang, J.H. Zhu, Z.G. Zou, New attempt at directly generating superbasicity on mesoporous silica SBA-15, Inorganic Chemistry 47 (2008) 4199–4208.

[23] C.F. Zhou, Y.M. Wang, Y. Cao, T.T. Zhuang, W. Huang, Y. Chun, J.H. Zhu, Solvent-free surface functionalized SBA-15 as a versatile trap of nitrosamines, Journal of Materials Chemistry 16 (2006) 1520–1528.

[24] C. Zhang, H. He, A comparative study of TiO_2 supported noble metal catalysts for the oxidation of formaldehyde at room temperature, Catalysis Today 126 (2007) 345–350.

[25] L. Wang, M. Sakurai, H. Kameyama, Study of catalytic decomposition of formaldehyde on Pt/TiO_2 alumite catalyst at ambient temperature, Journal of Hazardous Materials 167 (2009) 399–405.

[26] A.D. Allian, K. Takanabe, K.L. Fujdala, X. Hao, T.J. Truex, J. Cai, C. Buda, M. Neurock, E. Iglesia, Chemisorption of CO and mechanism of CO oxidation on supported platinum nanoclusters, Journal of the American Chemical Society 133 (2011) 4498–4517.

[27] Y. Liu, C.J. Jia, J. Yamasahi, O. Terasaki, F. Schuth, Highly active iron oxide supported gold catalysts for CO oxidation: how small

must the gold nanoparticles be?, Angewandte Chemie-International Edition 49 (2010) 1–6
[28] A. Iyer, H. Galindo, S. Sithambaram, C. King'ondu, C.H. Chen, S.L. Suib, Nanoscale manganese oxide octahedral molecular sieves (OMS-2) as efficient photocatalysts in 2-propanol oxidation, Applied Catalysis A 375 (2010) 295–302.
[29] T. Daubert, R. Danner (Eds.), Hemisphere Publishing Corporation, 1976.
[30] N. Kijima, T. Ikeda, K. Oikawa, F. Izumi, Y. Yoshimura, J Crystal structure of an open-tunnel oxide α-MnO_2 analyzed by Rietveld refinements and MEM-based pattern fitting, Journal of Solid State Chemistry 177 (2004) 1258–1267.
[31] A.R. Gandhe, J.S. Rebello, J.L. Figueiredo, J.B. Fernandes, Manganese oxide OMS-2 as an effective catalyst for total oxidation of ethyl acetate, Applied Catalysis B 72 (2007) 129–135.